Supporting Information

Electrochemical Driven Water Oxidation by Molecular Catalysts *in situ* Polymerized on the Surface of Graphite Carbon Electrode

Lei Wang,[a] Ke Fan,[a] Quentin Daniel,[a] Lele Duan,[a] Fusheng Li,[a] Bertrand Philippe,[b] Håkan Rensmo,[b] Hong Chen,[c] Junliang Sun[c] and Licheng Sun*[ad]

[a] Department of Chemistry, KTH Royal Institute of Technology, 10044 Stockholm, Sweden. E-mail: lichengs@kth.se

[b] Department of Physics and Astronomy, Uppsala University, Box 516, 751 20, Uppsala, Sweden

[c] Berzelii Center EXSELENT on Porous Materials and Department of Materials and Environmental Chemistry, Stockholm University, 106 91 Stockholm, Sweden

[d] State Key Laboratory of Fine Chemicals, DUT–KTH Joint Education and Research Center on Molecular Devices, Dalian University of Technology (DUT), Dalian 116024, P. R. China

Reagents and Instruments

Cis-$Ru(DMSO)_4Cl_2$, ligands 4-(2-(1H-pyrrol-1-yl)ethyl)pyridine and 4-(3-(1H-pyrrol-1-yl)propyl)pyridine were prepared according to published methods.[1,2] Other compounds and solvents were purchased from Aldrich and used without further purification. Water used in syntheses and measurements was deionized by Milli-Q technique.^{1}H NMR spectra were recorded with a Bruker Advance 500 spectrometer. Mass spectrometry measurements were performed on a Finnigan LCQ Advantage MAX mass spectrometer.High resolution mass spectra were performed by electrospray ionization (ESI) on an HP 1100 MSD instrument. Electrochemistry measurements: Cyclic Voltammograms (CVs) and Differential Pulse Voltammetry (DPV) were carried out with an Autolab potential station with a GPES electrochemical interface (Eco Chemie). Pyrolytic Graphite Electrode (Basal Plane, OD: 6 mm, ID: 3.0 mm, purchased from BAS Inc, Japan) as working electrode, a platinum column as the counter−electrode, and a Ag/AgCl electrode (3 M KCl; 190 mV vs. NHE) as the reference electrode in aqueous, $Ag/AgNO_3$ electrode (0.1 M $AgNO_3$ in CH_3CN; 350 mV vs.NHE). The oxygen was detected by Gas Chromatography-2014 (SHIMADZU), using He as carrying gas. Energy dispersive X-ray spectroscopy was recorded on JEOL JSM-7000F microscope operated at 15 kV. X-ray photoelectron spectroscopy (XPS) were recorded with an ESCA 300 (hv = 1486.6 eV).

Synthesis.

4-(2-(1H-pyrrol-1-yl)ethyl)pyridine. The procedure was followed as reference.[2] 4-pyridinethanol(also 4-Pyridinepropanol) was heated to flux in HBr solution for 8 h, then after the solution cooled to room

temperature, the resulted solution was neutralized with 6 M KOH, and the mixture was extracted by chloroform (3×100 mL), combine the organic phase and dry it with Na_2SO_4 overnight. The solvent was removed by rotary evaporation, and the brown oil product was used without further purification. 4-(2-bromoethyl)pyridine (370 mg, 2 mmol) and 1-H pyrrole (335 mg, 5 mmol) were mixed in a 25 ml round flask with 10 ml DMF under N_2, and 1.34 g K_2CO_3 was added, the mixture was kept stirring at 100℃ for 6 h. The solvent was removed under vacuum, and the raw product was purified by column chromatography over silica gel. The product was afforded as yellowish powder (310 mg, 90 % yield). ^{1}H-NMR (500 MHz, $CDCl_3$): 8.48 (d, 2 H), 7.01 (d, 2H), 6.55 (t, 2H); 6.11 (t, 2H); 4.12 (t, 2H); 3.06 (t, 2H). MS (ESI): calcd for 173.11 ($M + H^+$), found m/z^+ = 172.96.

4-(3-(1H-pyrrol-1-yl) propyl) pyridine. The product was afforded as yellow oil (82% yield). ^{1}H-NMR (500 MHz, $CDCl_3$): 8.51 (d, 2 H), 7.10 (d, 2H), 6.65 (t, 2H); 6.17 (t, 2H); 3.91 (t, 2H); 2.58 (t, 2H); 2.12 (m, 2H). MS (ESI): calcd for 187.12 ($M + H^+$), found m/z^+ = 187.36.

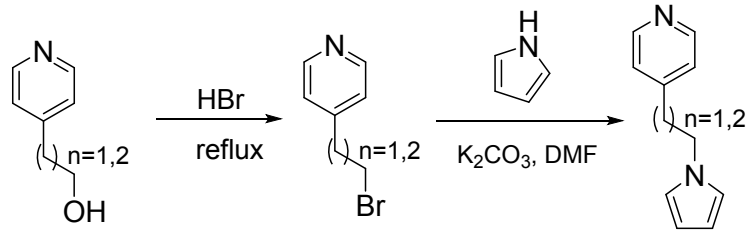

Complex 1. A mixture of 2,2′ −bipyridine−6,6′ −dicarboxylic acid (H_2bda) (100 mg, 0.41 mmol), cis−[Ru(DMSO)$_4$Cl$_2$] (200 mg, 0.41 mmol) and triethylamine (0.3 mL) in methanol (20 mL) was degassed with N_2 and refluxed over 4 hours. The suspension solution obtained was filtered, the resulting solid (100 mg, 0.2 mmol) without further purification was dissolved in 10 mL methanol (0.1 mL DMSO) with 1 equivalent of 4−iodopyridine (41 mg, 0. 2 mmol), and the solution was heated to 40 ℃ under N_2 protection for 5 min, then 1 equivalent another axial ligand was added, and the mixture was refluxed for 4 h, then the solvent was removed. The rest solid was purified by column chromatography on silica gel using methanol and dichloromethane mixture (1:15, v: v) as eluents. The product was afforded as dark red powder (87 mg, 60% yield). ^{1}H-NMR (500 MHz, MeOD, $CDCl_3$, Ascorbic acid): 8.43 (t, 2 H), 7.96 (d, 2H), 7.80 (t, 2H); 7.52 (d, 2H); 7.46 (t, 2H); 7.36 (d, 2H);6.72 (d, 2H); 6.36 (s, 2H); 5.86 (d, 2H); 3.96 (t, 2H); 2.87 (t, 2H). MS (ESI): calcd for 721.9838 ($M + H^+$), found m/z^+ = 721.7695.

Complex 2. The product was afforded as dark red powder (97 mg, 66% yield).^{1}H-NMR (500 MHz, MeOD, $CDCl_3$, Ascorbic acid): 8.45 (d, 2 H), 7.96 (d, 2H), 7.79 (t, 2H); 7.54 (d, 2H); 7.47 (d, 2H); 7.37 (d, 2H);6.88 (d, 2H); 6.46 (s, 2H); 5.87 (s, 2H); 3.76 (t, 2H); 2.39 (t, 2H)); 1.86 (m, 2H). MS (ESI): calcd for 735.9995 ($M + H^+$), found m/z^+ = 735.8263.

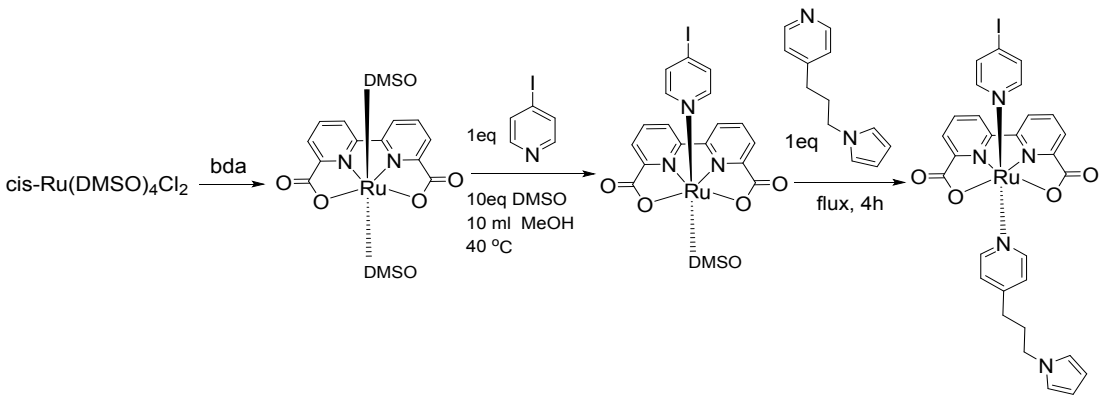

Functionalization of the BPG Electrode

The oxidizing polymerization of complexes **1** and **2**were carried out on two pyrolytic graphite electrodes (basal plane, diameter 3mm) (BPG) respectively, through a 20 times of successive cyclic voltammograms (CVs) in a relatively high concentration (10^{-2} M for both **1** and **2**) of catalyst in a CH_3CN (20% CF_3CH_2OH) solution (0.1 M $LiClO_4$ as electrolyte) from the range of 0 to 1.0 V vs. $Ag/AgNO_3$. After modification, the working electrodes were thoroughly rinsed with ethanol and water to remove any physically adsorbed compounds.

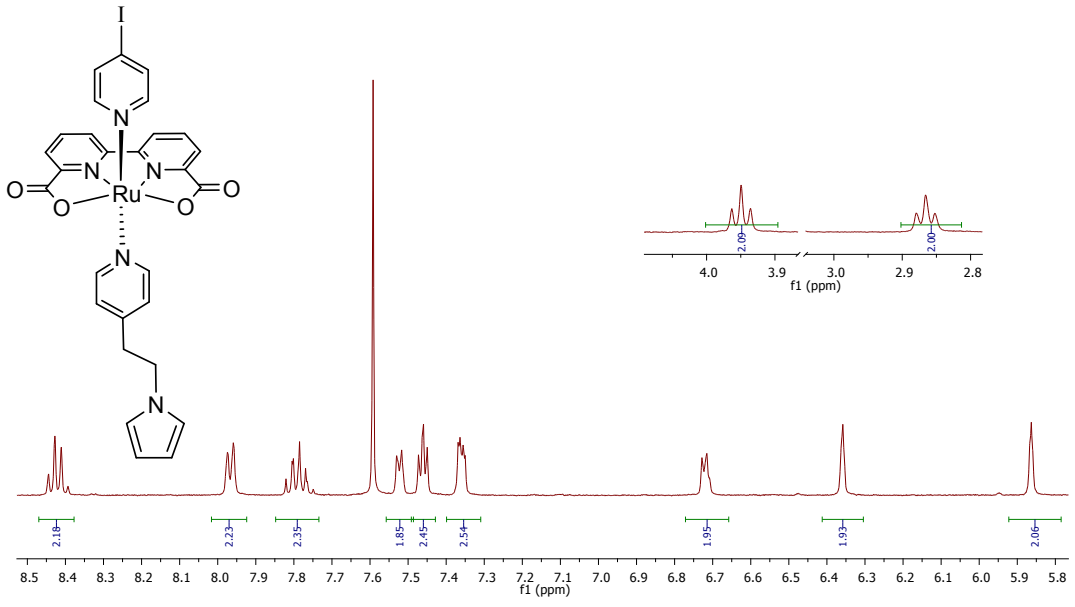

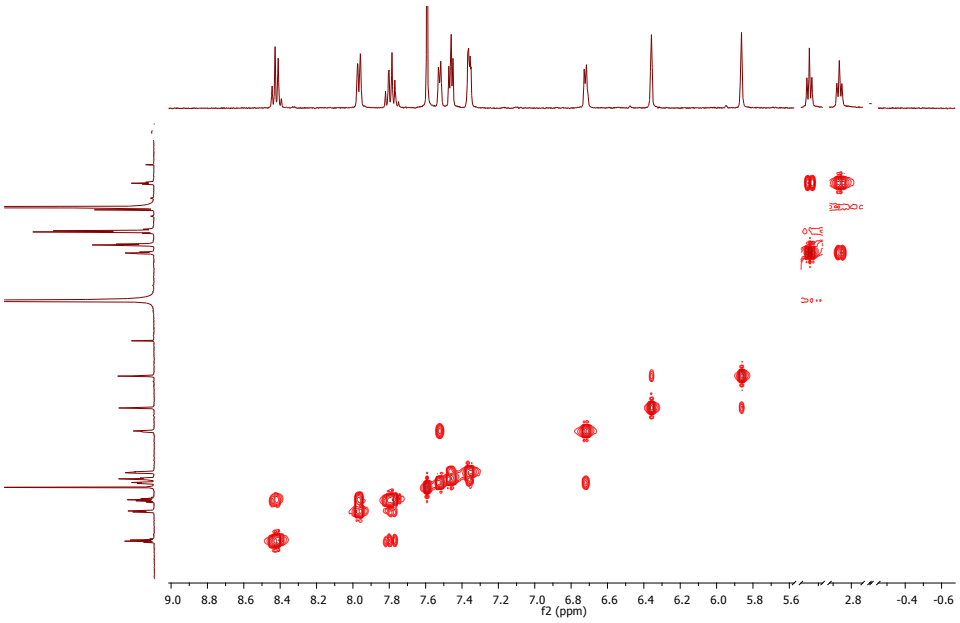
9.0 8.8 8.6 8.4 8.2 8.0 7.8 7.6 7.4 7.2 7.0 6.8 6.6 6.4 6.2 6.0 5.8 5.6 2.8 -0.4 -0.6
f2 (ppm)

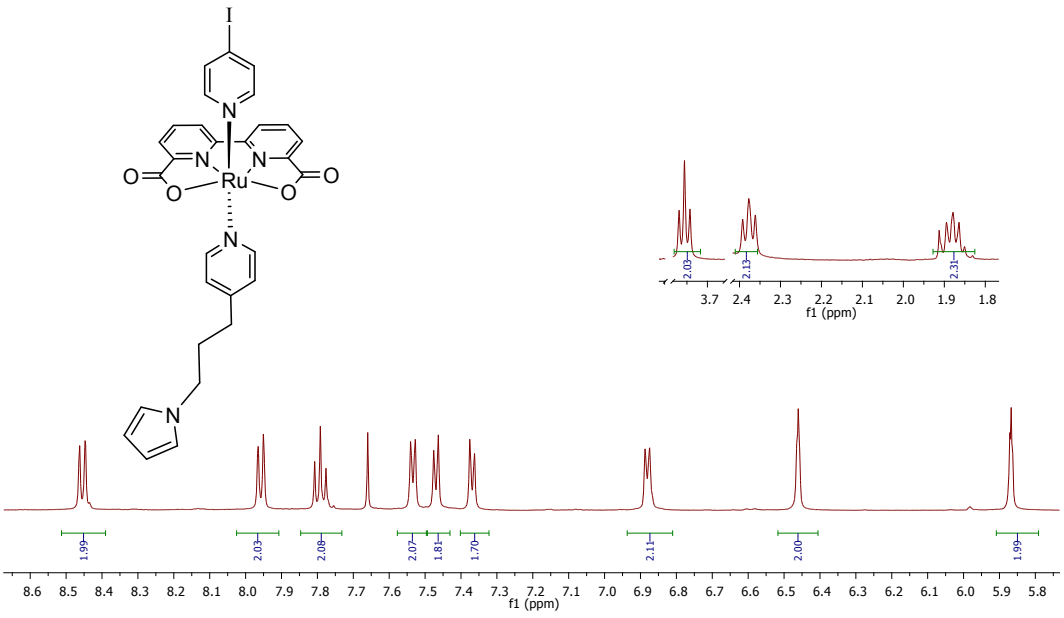
I
N
O
O
N
Ru
N
O
O
N
N
1.99
2.03
2.08
2.07
1.81
1.70
2.11
2.00
1.99
8.6 8.5 8.4 8.3 8.2 8.1 8.0 7.9 7.8 7.7 7.6 7.5 7.4 7.3 7.2 7.1 7.0 6.9 6.8 6.7 6.6 6.5 6.4 6.3 6.2 6.1 6.0 5.9 5.8
f1 (ppm)

2.03
2.13
2.31
3.7 2.4 2.3 2.2 2.1 2.0 1.9 1.8
f1 (ppm)

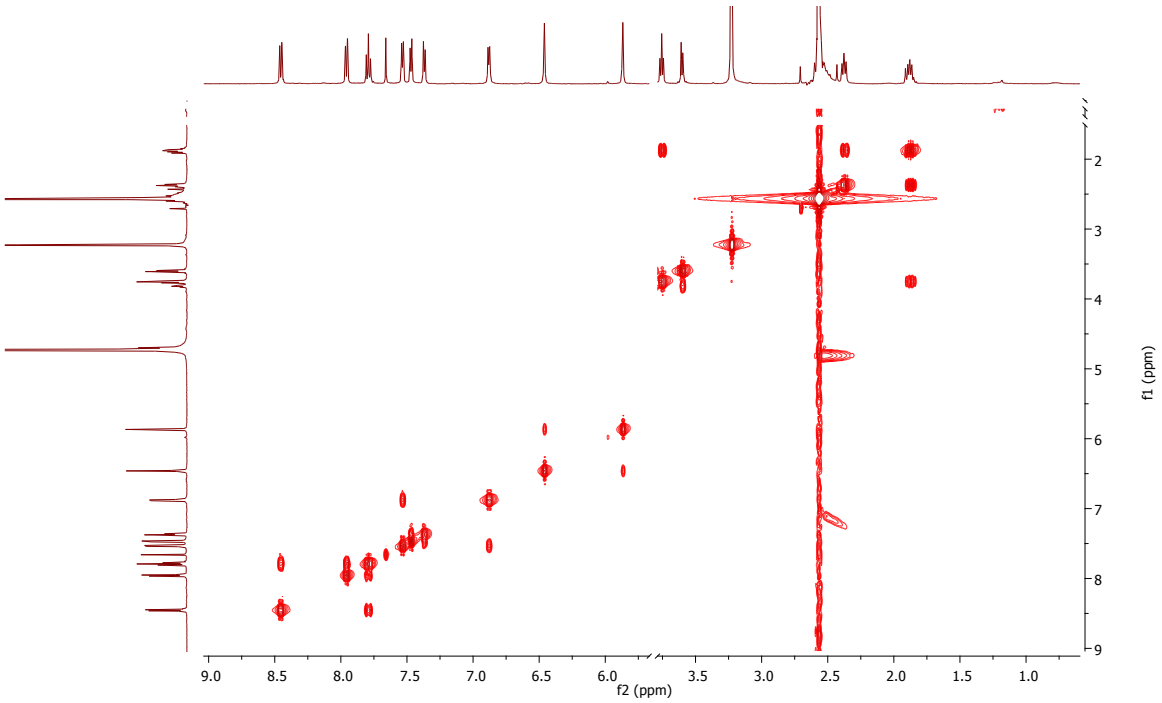

Figure S1. ^{1}H and H-H COSY NMR spectra of complex **1** and **2**. For these complexes, the equatorial has strong electron donating ability, that caused these Ru^{II} complexes oxidized to paramagnetic Ru^{III} species by air at room temperature, and cause difficulty to characterize by ^{1}H NMR. However, using ascorbic acid as the reductant could solve this problem to obtain sharp signals.

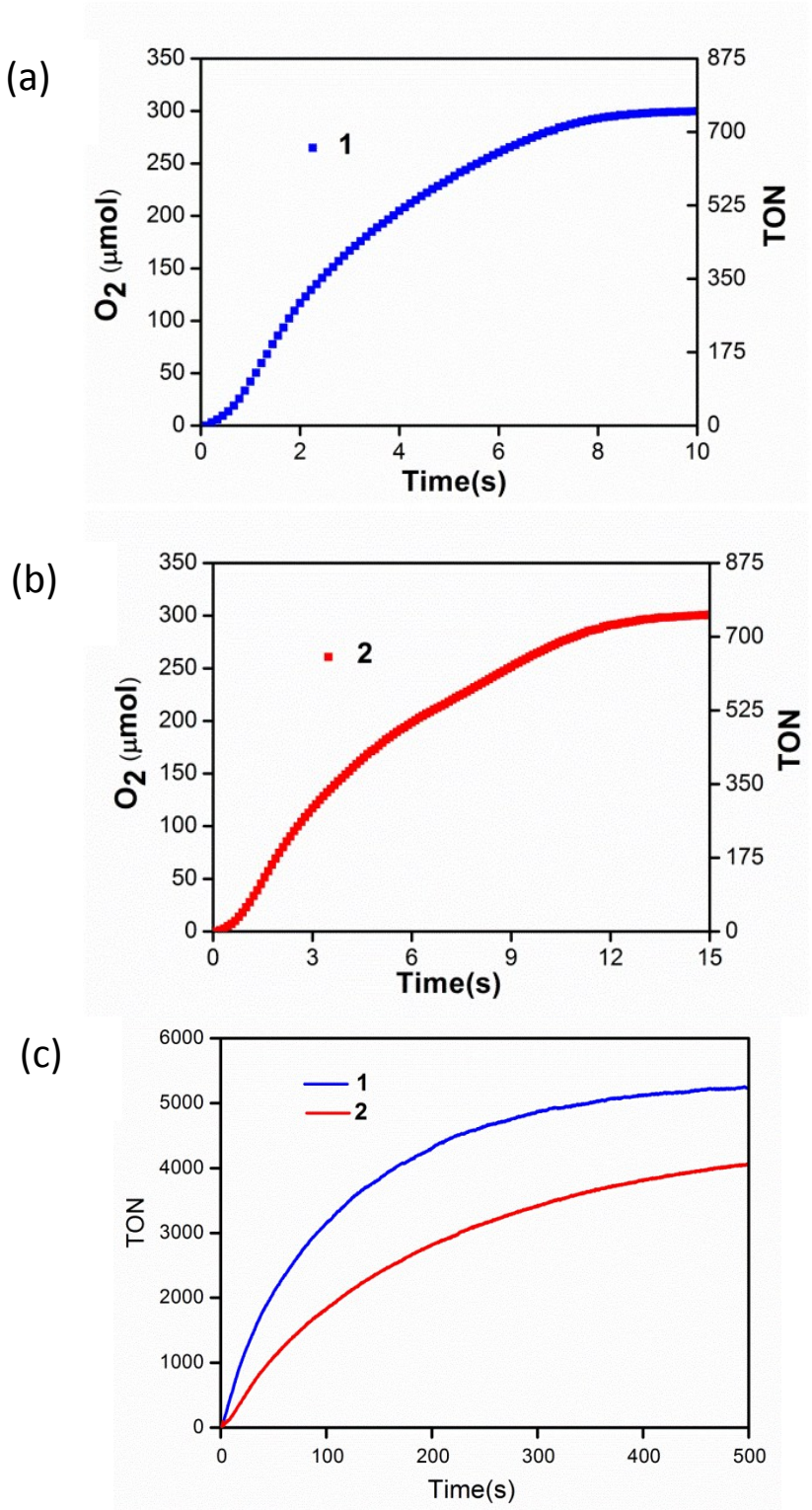

Figure S2. Curves of oxygen evolution recorded in the gas phase with pressure sensor and calibrated by GC. Conditions: an aqueous solution of HNO_3 (initial pH 1.0, 3.5 mL) containing Ce^{IV} 0.365 M. (a) [**1**] = 1.14 $\times 10^{-4}$ M, the corresponding initial TOF (**1**) = 190 ± 13; (b) [**2**] = 1.14 $\times 10^{-4}$ M, TOF (**2**) = 126 ± 18; (c) [**1**] = [**2**] = 1.5 $\times 10^{-5}$M, the TON of complex **1** (5360 ± 289)in 500 seconds shows higher TON than **2** (4420 ± 236).

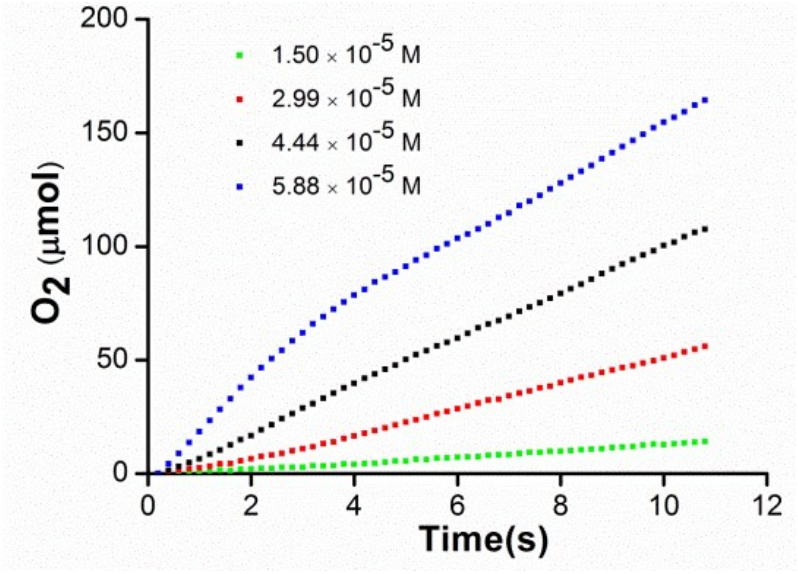

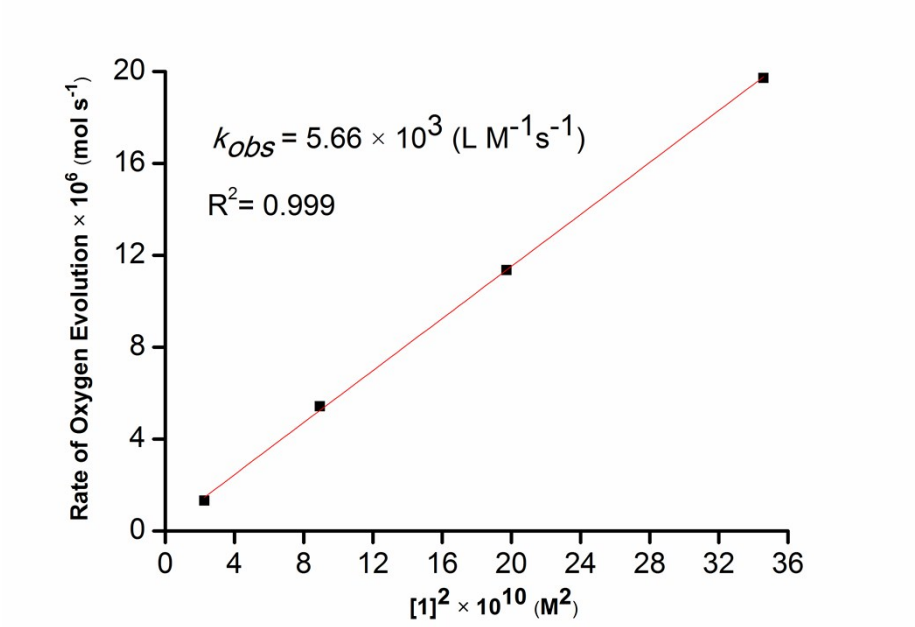

Figure S3. Upper: Plots of O_2 evolution vs time at various concentrations of complexes **1** in pH 1.0 of HNO_3 containing Ce^{IV}. Below: Plots of k_{obs} (the initial rates were calculated by linear fitting the data from 0 to 10 s) versus $[\mathbf{1}]^2$. Second order rate constant 5.66×10^3 ($LM^{-1}s^{-1}$) was obtained regards with **1**. Additionally, the estimated overpotential of Ce^{IV} at pH 1 was ~ 500 mV.

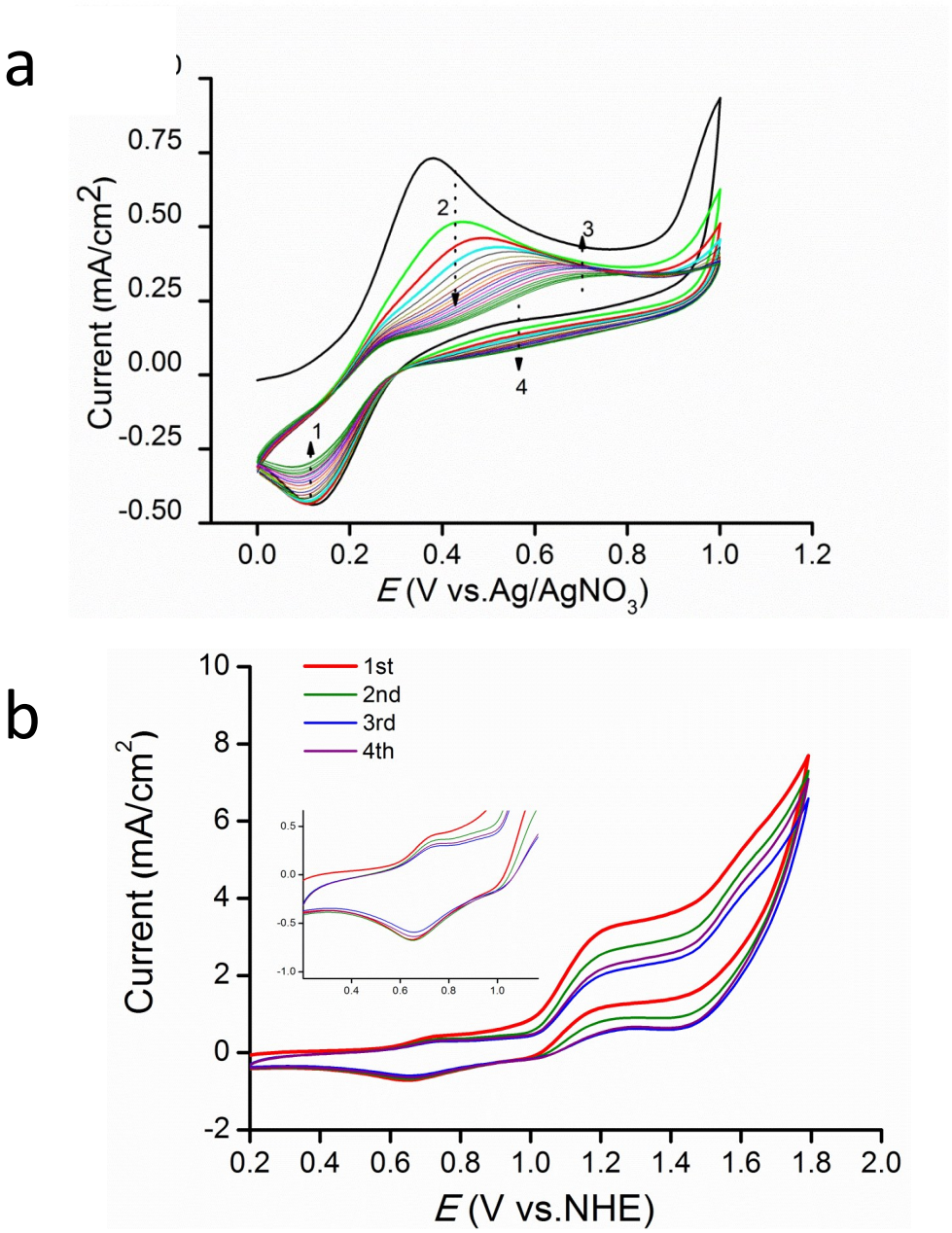

Figure S4. a) Electro-polymerization was carried out by running successive cyclic voltammograms of a 10^{-2} M solution of complex **1** in CH_3CN containing 20% of CF_3CH_2OH and 0.1 M $LiClO_4$, WE: PGBE.CE: platinum column, and RE: $Ag/AgNO_3$. b) Four consecutive CVs of **1**@BPG in aqueous solution (pH 7.2) after immobilization.

The decreasing of the peak current is an unusual phenomenon. Here we give a hypothesis: (1) first of all, the peak current was mainly contribute by polypyrrole; (2) after polymerization of the monomer onto the surface of the electrode, the bulk Ru catalyst tail which is unconducive will possibly inhibit the further polymerization. Based on (1) and (2) above, by increasing the scan numbers, less and less monomer can be immobilized on to the surface which resulted the decreasing of the peak current.

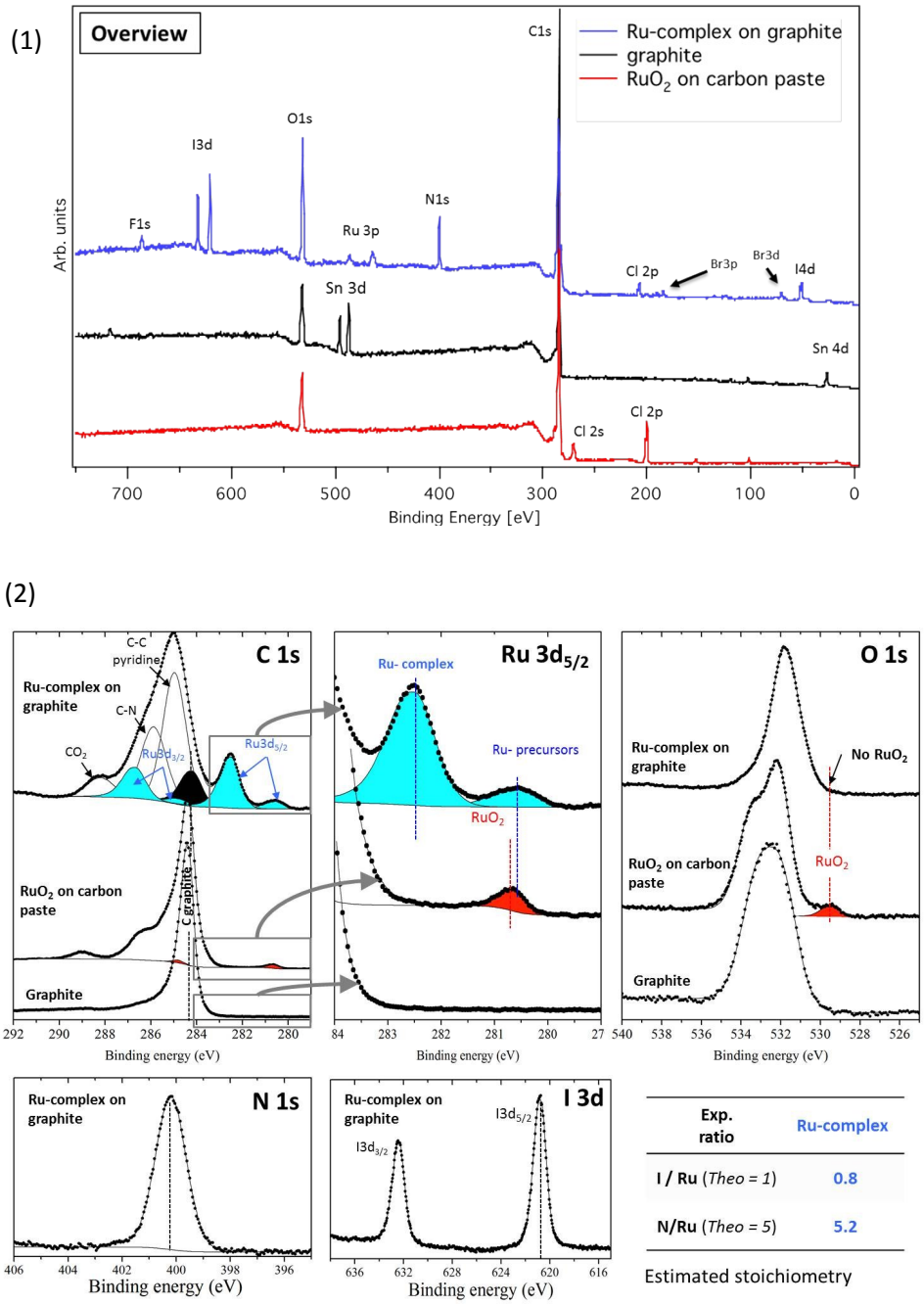

Figure S5. XPS measurements on three samples: the pristine graphite surface, RuO_2 on graphite paste and the immobilized complex **1** on graphite surface. (1) Overview of the spectra; (2) C1s, $Ru3d_{5/2}$, O1s, N1s and I3d core level spectra of the Ru-complex on graphite. The spectra of RuO_2 on the graphite substrate are presented as comparison. The presence of RuO_2 can be excluded as the typical O1s core level peak of RuO_2 at 529.4 eV (Ru 2p at 280.7eV) cannot be observed on the sample containing the Ru-complex[3]. In addition, the ruthenium (Ru II and Ru III) presents in the catalyst is very distinguishable with a characteristic $Ru2p_{5/2}$ core peak at higher binding energy (282.5 eV) due to the acceptor nature of the ligands[4]. A single N1s core peak can be detected at 400.2 eV in agreement with the similar chemical environments (C-**N**-C) of the five nitrogen of the catalyst. A single $I3d_{5/2}$ core peak is also detected in perfect agreement with the molecule synthesized. Finally the N/Ru and I/Ru atomic ratio have been determined and are very close to the theoretical one suggested by the molecule, i.e. 5.2 (5) and 0.8 (1), respectively. The observed "Ru- precursors" which is clearly not Ru oxide, may due to the ligand exchange of the Ru complex.

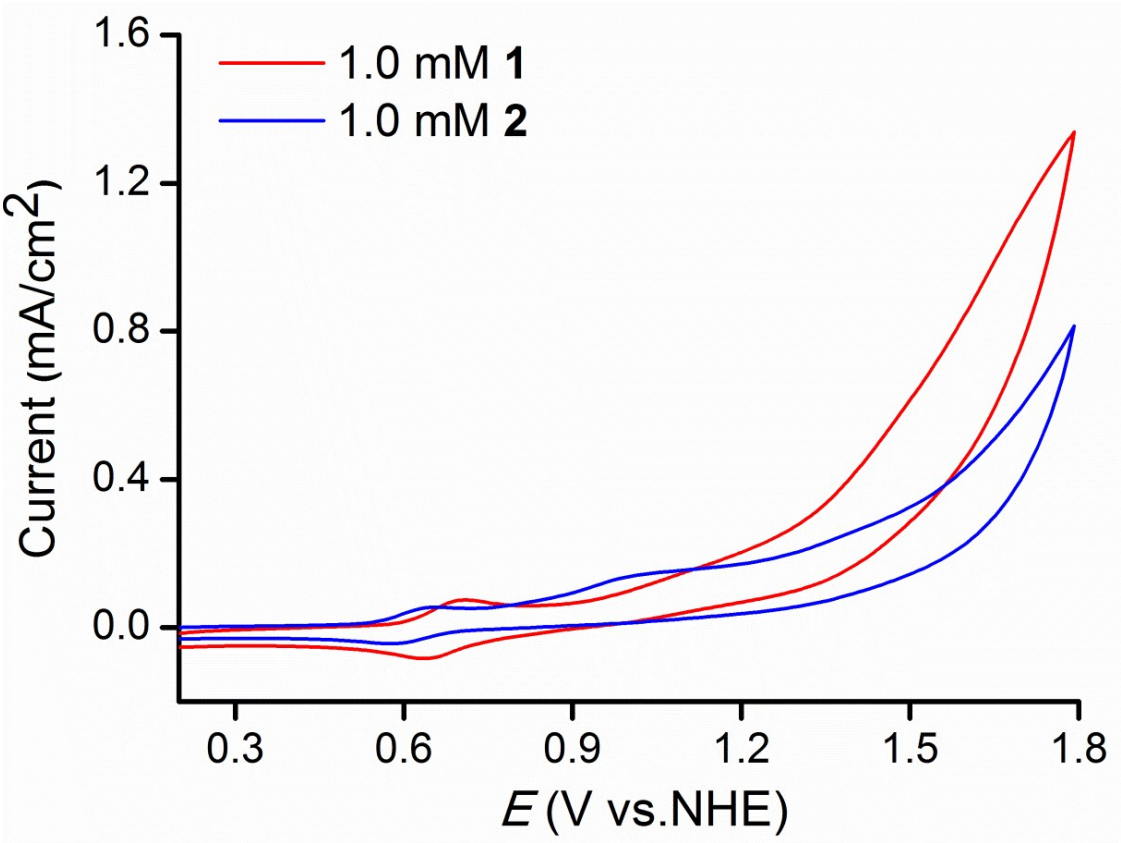

Figure S6. Homogeneous catalysts in solution: CV curves of the 1.0 mM **1**(red line) and **2**(blue line). Conditions: aqueous (pH 7.2 phosphate buffer solution, 0.1 M) containing 20% CF_3CH_2OH (co-solvent for dissolving the Ru complexes), scan rate: 100 mV s^{-1}, room temperature.

Table S1. Peak potentials of complexes **1** and **2** before (homogenous catalysis) and after immobilization. RuO_2 was also measured as a reference. All of the potentials are *vs.* to NHE.

Complex	$Ru^{III/II}$ (V)	$Ru^{IV/III}$ (V)	$Ru^{V/IV}$ (V)
1	0.665	0.849	1.021
2	0.636	0.864	1.032
1@BPG	0.688	0.850	1.066
2@BPG	0.672	0.864	1.058
RuO_2	0.474	0.690	0.937

In order to make a better comparison, here we made a RuO_2 electrode by immobilize carbon paste which contain 10wt% of RuO_2 on conductive glass. The DPVs of RuO_2 was shown in Figure S6.

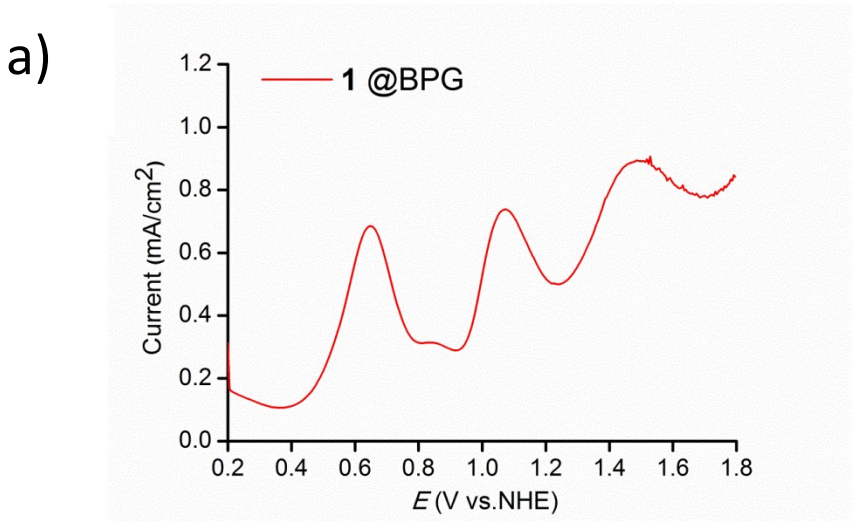

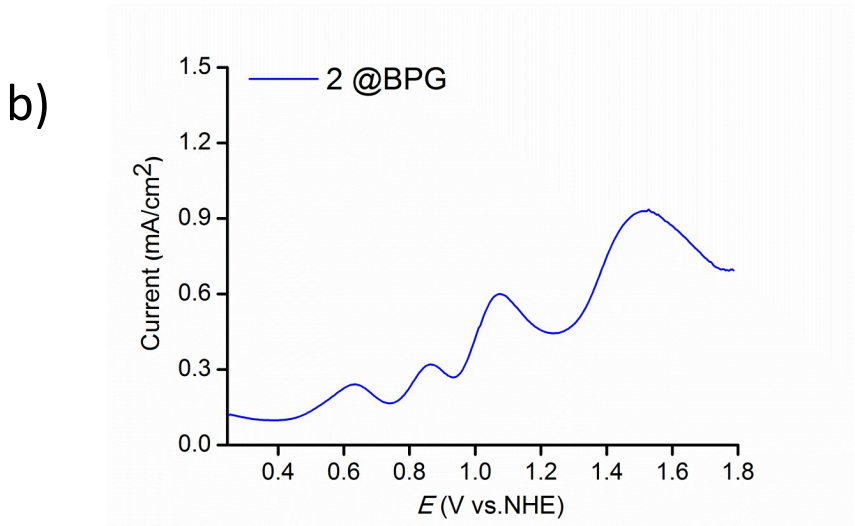

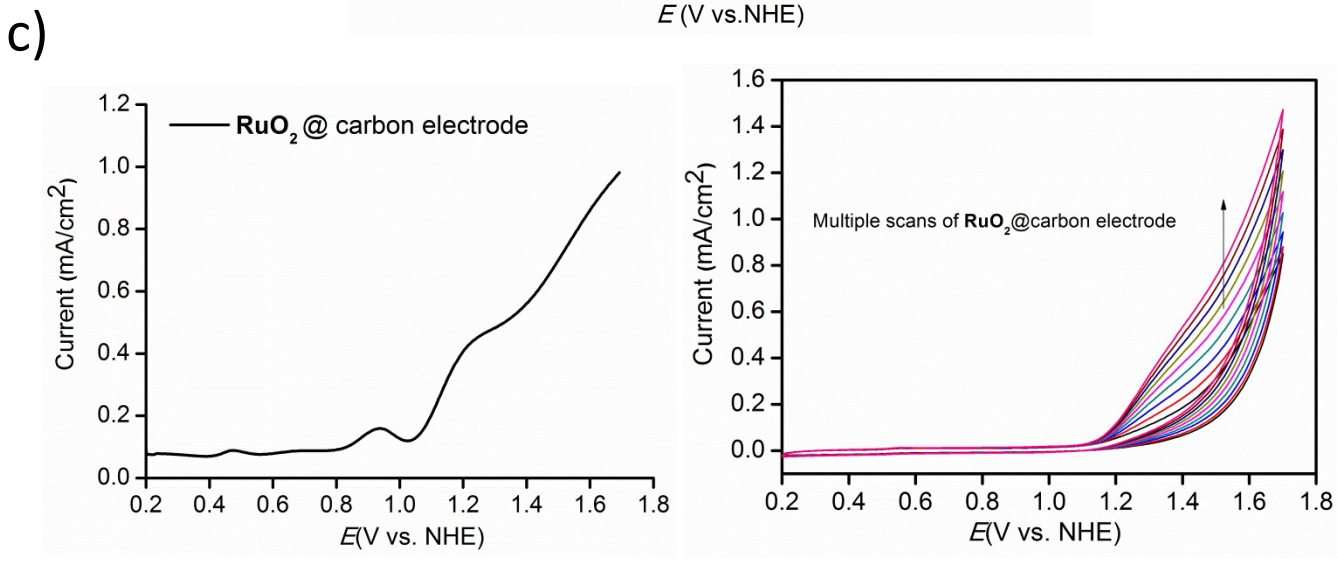

Figure S7. a): DPV (Differential Pulse Voltammetry) curve of **1**@BPG in pH 7.2 phosphate buffer (0.1 M). b): DPV curve of **2**@BPG in pH 7.2 phosphate buffer (0.1 M). c): DPV and CVs curve of **RuO_2**@carbon electrode in pH 7.2 phosphate buffer (0.1 M).

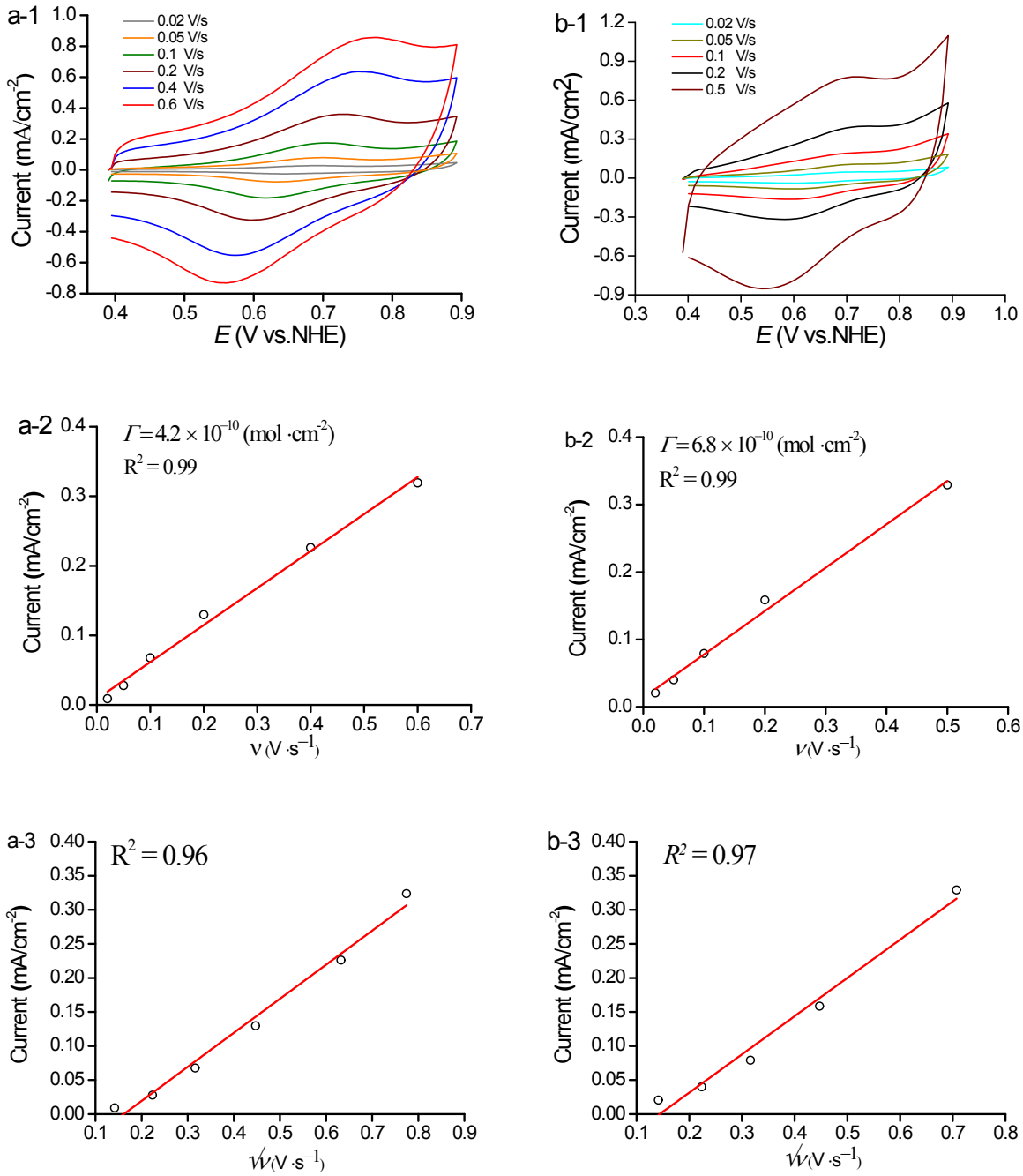

Figure S8. a-1: CV curves of **1**@BPG at different scan rates; conditions: pH 7 phosphate buffer (0.1 M), $\Gamma_1 = 4.2 \times 10^{-10}$ mol cm^{-2}. a-2: dependence of peak current on different scan rates, a-3: dependence of peak current on square root of scan rate. a-2 shows better linearity than a-3, indicating the catalyst is immobilized on the surface. b-1, b-2 and b-3show the $\Gamma$of complex **2**, $\Gamma_2 = 6.8 \times 10^{-10}$ mol cm^{-2}.

$$\Gamma = \frac{4RT}{n^2F^2A} Slope \qquad \textbf{S1}$$

Where F (Faraday's constant) = 96485, n = electrons transfer number = 1, R (ideal gas constant) = 8.314 JK^{-1}mol^{-1}, T = 298 K, A = electrode surface area (cm^2), Γ= surface catalyst loading (mol/cm^2), current (A), scan rate ν (V/s).

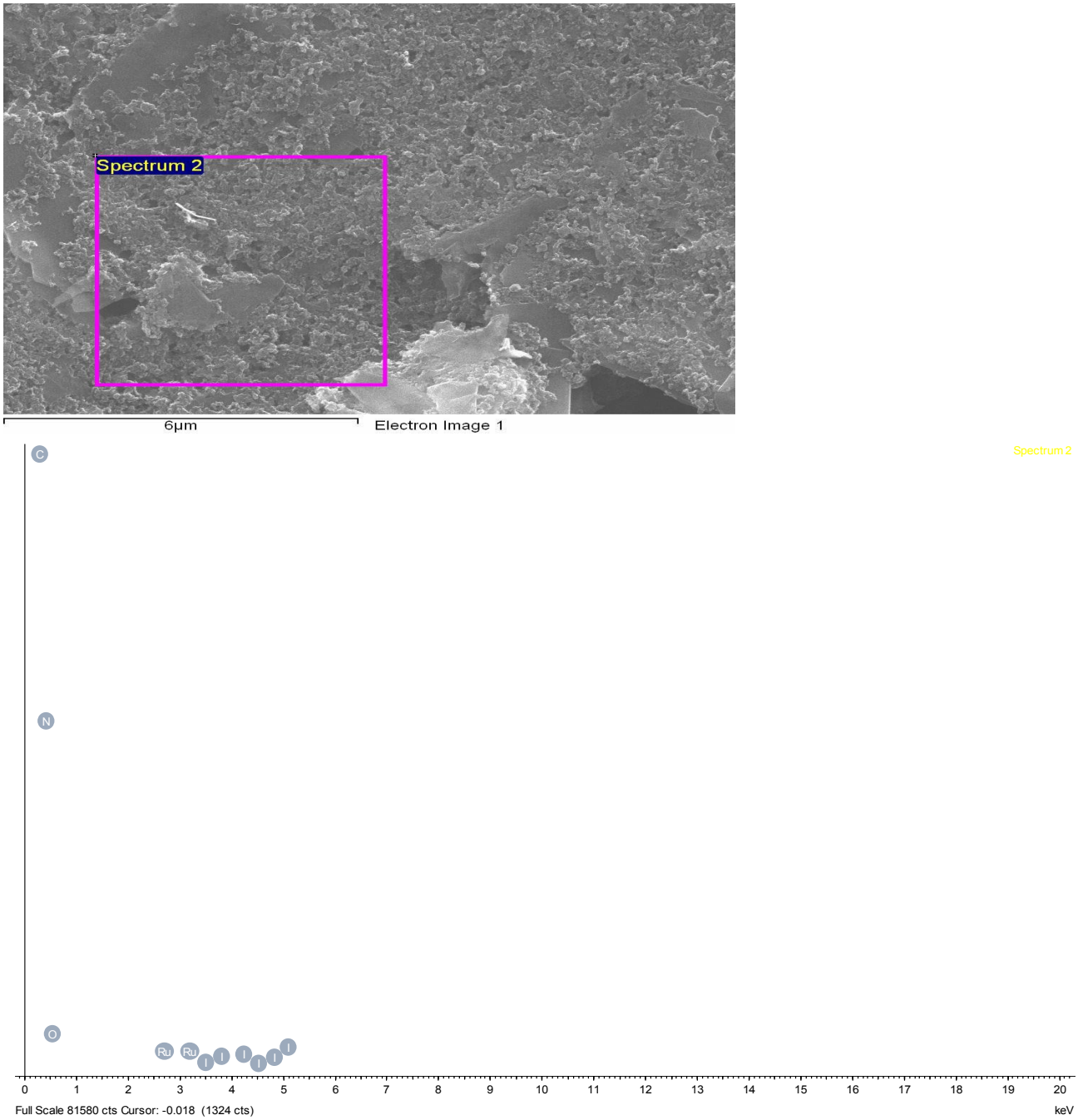

Figure S9. Energy dispersive X-ray spectroscopy (EDX) of **1**@BPG shows the surface loading of the Ru catalysts.

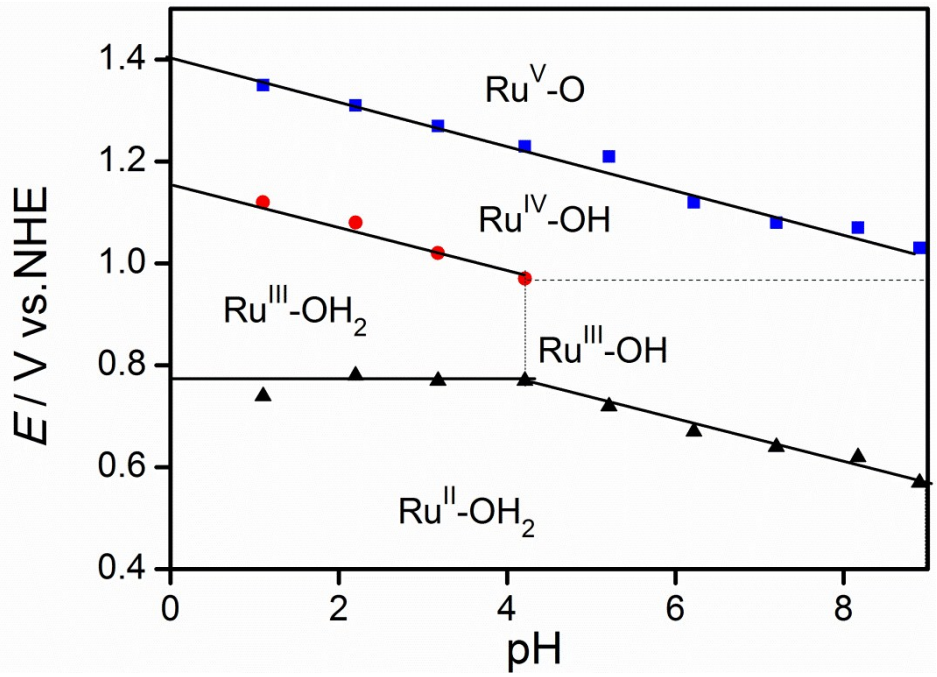

Figure S10. Pourbaix diagram of **1**@BPG, recorded in aqueous solutions, all of the Ru species are proposed according to the PCET (proton coupling electron transfer) behavior.

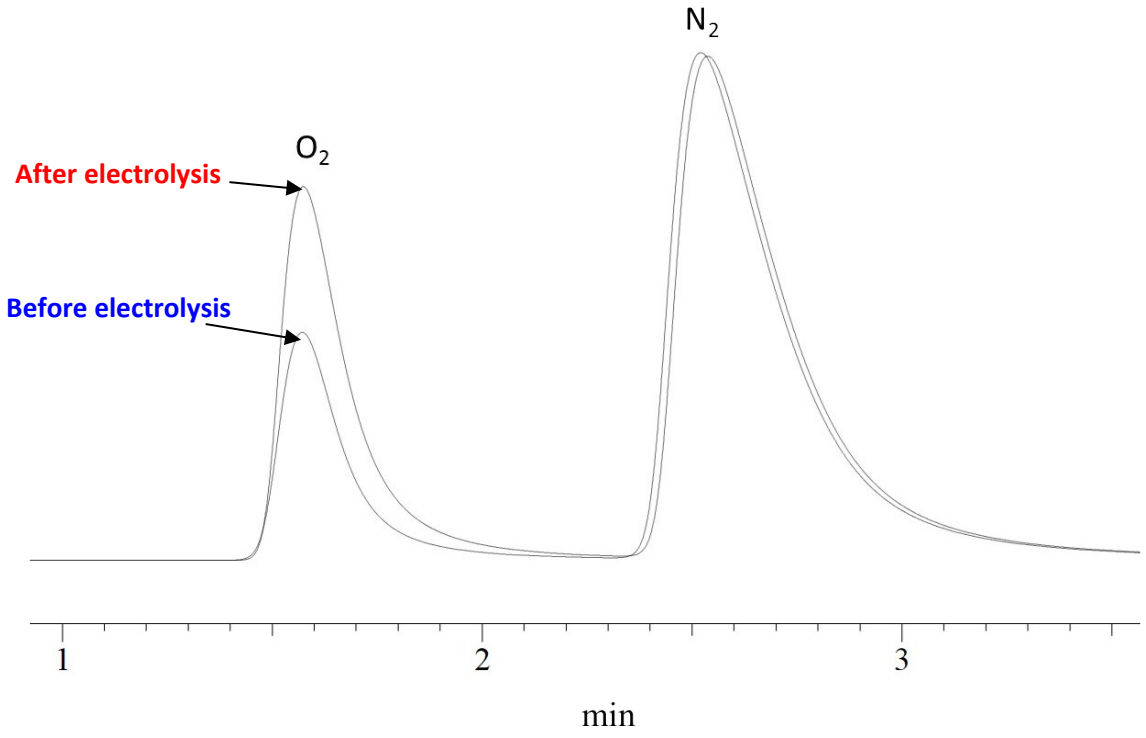

Figure S11. Gas chromatographic traces before and after electrolysis show the generated oxygen for **1**@BPG.

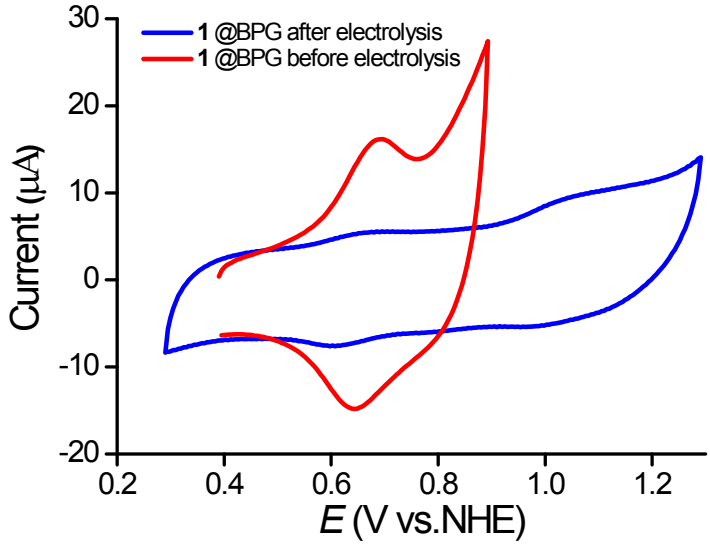

Figure S12. CVs of the redox waves of **1**@BPG before (red) and after (blue) 1 hour of bulk electrolysis. After electrolysis, the peak current of the redox wave was dropped dramatically, indicating the catalyst dissociation happened during the electrolysis which resulted a decreasing of the activity (Figure 4).

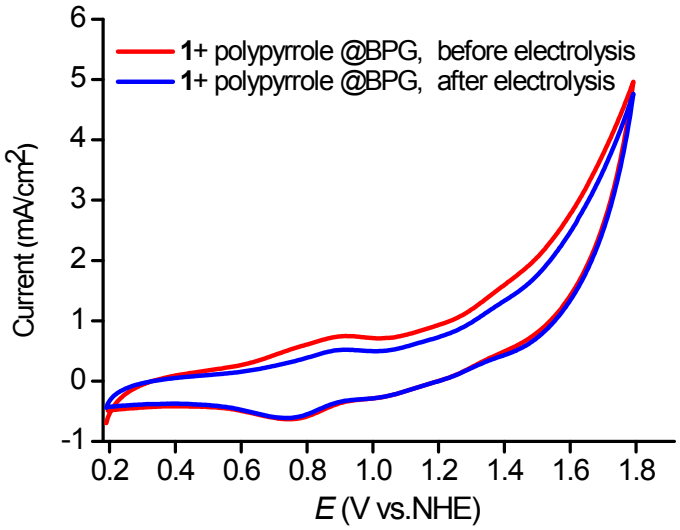

Figure S13. CVs of the redox waves of **1** + polypyrrole @BPG before (red) and after (blue) bulk electrolysis. The minor changes indicating the catalyst was stable on the surface.

References

[1]E. Duliere, M. Devillers and J. Marchand-Brynaert, *Organometallics*, **2003**, 22, 804-811.

[2] Lang, R.; Shi, L.; Li, D.; Xia, C.; Li, F. *Organic Letters* **2012**, 14, 4130.

[3] K. S. Kim, N. Winograd. *J. of Catalysis*, **1974**, 35, 66-72

[4] Rex E. Shepherd and Terry K. Myser al. *Inorganic Chemistry* **1987** *26* (15), 2440-2444.